Kazakeviciute-Makovska, R.; Heuchel, M.; Kratz, K.; Steeb, H.:

Universal relations in linear thermoelastic theories of thermally-responsive shape memory polymers

In: International Journal of Engineering Science (2014) Elsevier

DOI: 10.1016/j.ijengsci.2014.05.009

Journal of the Mechanics and Physics of Solids

" *... universal results of various kinds are road signs posted to direct and to warn the experimenter in his exploration of the constitutive properties of real materials*".

M. F. Beatty (1987)

Universal relations in linear thermoelastic theories of thermally-responsive shape memory polymers

R. Kazakevičiūtė-Makovska,[1)] M. Heuchel,[2)] K. Kratz[2)], H. Steeb,[1)]

[1)] Ruhr University Bochum, Institute of Mechanics,
Universitätsstr. 150 D-44780 Bochum, Germany
Email: *Rasa.Kazakeviciute-Makovska@ruhr-uni-bochum.de*, *Holger.Steeb@ruhr-uni-bochum.de*

[2)] Helmholtz-Zentrum Geesthacht (HZG)
Institute of Biomaterial Science
Kantstrasse 55, D-14513 Teltow, Germany
Email: *matthias.heuchel@hzg.de*, *karl.kratz@hzg.de*

Abstract In this paper we formulate an one-dimensional linear thermo-elastic (LTE) model in integral form for describing the behavior of thermally-responsive shape memory polymers (SMPs), which unifies and slightly generalizes numerous theories proposed in the literature starting with the seminal approach proposed by Liu et al. (2006). The presented model in its most general form requires the calibration of three response functions. Detailed analysis of four types of shape memory cycles (SMCs) used to quantify the shape memory effect in thermally-responsive SMPs and the corresponding forms of constitutive relations derived within LTE model display a number of critical properties. In particular, two of three response functions may be determined in many different ways from strain and stress storage/recovery profiles measured in SMCs (the third response function may be determined from an independent test). As implication of this fact, we show that the LTE model predicts a number of inter-relations between the measured strain and stress storage/recovery profiles. All these relations are universal in the sense that for any shape memory polymer, which may be correctly described by LTE model, the strain/stress storage/recovery profiles measured in SMCs must satisfy (at least approximately) these relations. Their role within the LTE model is analogous to the role of universal relations in the theory of finite deformation elasticity. In particular, these universal relationships provide a theoretical basis for the validation of any model within the LTE class. The basic theoretical results derived in this paper are illustrated using data obtained by Liu et al. (2006).

1. Introduction

Shape memory polymers (SMPs), including shape memory polymer nanocomposites (SMPNCs), are an emerging class of smart materials with potential applications ranging from biomedicine and nanoengineering to space technology [1 - 10]. Compared to shape memory alloys and ceramics, SMPs have many advantages such as low density, easy processing, high fixture strain and high strain-recovery ability, wide shape transition temperature, biocompatibility, and even relatively low cost [3, 5, 8, 10]. To assist an efficient design and use of SMP-based elements and devices, it is necessary to develop

- efficient experimental procedures for the characterization of mechanical, thermal, and functional properties of this class of materials,
- constitutive models that capture the key features of the behavior of SMPs subjected to arbitrary strain, stress, and temperature histories,
- reliable methods for the evaluation of the constitutive models to validate models prediction with experimental results,
- methodology for finding response functions in thermo-mechanical models and the calibration of material parameters from measurable data, and
- computational algorithms for the analysis of particular problems.

Experimental characterization of SMPs requires the determination of their mechanical (elastic and rheological) and thermal properties as well as the quantification of the shape-memory behavior [6, 9, 11 - 13]. The mechanical and thermal properties of SMPs may be determined from standard mechanical tests (tensile, shearing or bending) at different temperatures, the dynamic mechanical thermal analysis (DMTA) tests, etc.

The functional properties of SMPs are quantified by multi-step cyclic thermomechanical tests. Each cycle involves programming of a sample and the recovery of its permanent shape [6, 9, 11 - 13]. Depending on the instrument used in experiment, these tests can be performed in strain- or stress-controlled modes such as uniaxial tension, shearing or bending of suitable samples [9, 11 - 13]. For the dual-shape memory effect, it is usually sufficient to determine the extent of shape fixing (shape fixity) and the degree of recovery (shape recovery), both of which can be extracted from Shape Memory Cycle (SMC) tests. In such experiments, the deformation (or programming) can be conducted by applying a force (stress-controlled mode) or a target strain (strain-controlled mode). The stress free shape recovery, on the other hand, can be carried out by either continuously heating or holding a polymer at a constant temperature until the strain reaches an equilibrium value. These different types of the shape memory cycle generate slightly different and complementary data that are needed both for the characterization of the shape memory effect in polymers and the constitutive modeling of this effect.

Macroscopic constitutive models for thermally-responsive SMPs may be grouped in two broad classes under the names thermoelastic and visco-thermoelastic models, respectively. Both classes may further be divided into subclasses depending on the range of admitted strains (small or finite). A review of various constitutive models with the discussion of their advantages and deficiencies may be found in [6, 11, 14 - 17]. In this paper, we concern with the class of relatively simple models to which we refer as Liner Thermoelastic (LTE) models. All models in this class have their intrinsic limitations because time and rate effects are not considered. On the other side, more general models belonging to the second group are often too complex for technical applications. Moreover, some of these models involve a large number of material parameters having no clear physical interpretation and hence very difficult to calibrate [6, 11, 14, 15]. The reliable evaluation of the predictive ability of these models remains an open problem.

The first model in the LTE class has been developed by Liu et al. [18] for the uniaxial deformation state and subsequently extended by the same authors to general three-dimensional problems [19] . In the following years, the original Liu et al. model has been extensively discussed in the literature with numerous modifications and extensions [6, 14, 20 - 27]. Interesting enough, the analysis of that literature shows that many of these presumably improved models, when tested against the Liu et al. [18, 19] data, show a less accurate prediction than the original model. This observation calls for the efficient methodology of determination of response functions and material parameters in respective models directly from measurable data.

Liu et al. [18, 19] carried out a careful experimental program to calibrate their model. However, they have made a number of assumptions on response functions that greatly reduce the need of experimental data. In particular, they determined material constants in their model through curve fitting by using the strain recovery data without making use of the stress storage data. Chen and Lagoudas [20] attempted to calibrate the Liu et al. model by using experimental data obtained by Liu et al. with a somewhat different methodology. Specifically, they do not use the above-mentioned assumptions and attempt to determine the response functions with full use of experimental data for all stress/strain storage/recovery profiles measured in strain-controlled SMCs. In particular, they used both the stress measurements during cooling and the strain measurements during heating. These measurements in the whole temperature range have been fully utilized since they make no assumptions on the form of the response functions. In fact, Chen and Lagoudas [20] have shown that it is possible to use their approach to assess the reasonableness of the assumptions made in Liu et al. [18, 19]. It is rather surprising to see that the theoretical results obtained by Chen and Lagoudas are actually less accurate than the theoretical solutions obtained by Liu et al. In fact, the results of [20] coincide very nicely with the Liu et al. data for the stress storage and unconstrained strain recovery profiles (Figs 4-7 of [20]). However, there is a far less good agreement of their results with data for the stress recovery profile (Fig. 8 of [20]).

In this work, we present a thermomechanically based formulation of the integral constitutive equation (LTE model) for SMPs that relates arbitrary strain, stress, and temperature histories under the assumption that strains are small and time rate effects may be neglected. We next show that the proposed constitutive law unifies and substantially generalizes various models for SMPs, which have been developed following the seminal papers by Liu et al. [18, 19]. The presented model contains only three well-defined response functions that can be identified experimentally from standard shape memory cycles (SMCs). To this end, we first briefly discuss in Section 2 different types of SMCs used to quantify the shape memory properties of polymers. In Section 3, we give a compact summary of the LTE constitutive models, which includes the original Liu model as well as numerous modifications of this model proposed in the literature. The developed general theory is used in Section 4 for the simulation of the complete SMCs in both strain- and stress-controlled mode. In Section 5, we present a methodology for obtaining the response functions in the LTE model directly from the measured strain/stress storage/recovery profiles in four different types of SMCs. In Section 6, it is shown that within LTE model there exist certain theoretical interrelationships between measurable strain and stress profiles. These relations play an analogous role as the well-known universal relationships in the theory of finite elasticity (see Beatty [28], Hayes and Knops [29], Pucci and Saccomandi [30]). In particular, the derived relations serve to test limitations in the predictive capability of LTE models and they may be used to valuate several factors influencing the optimal behavior of SMPs.

2. Characterization of the shape memory effect

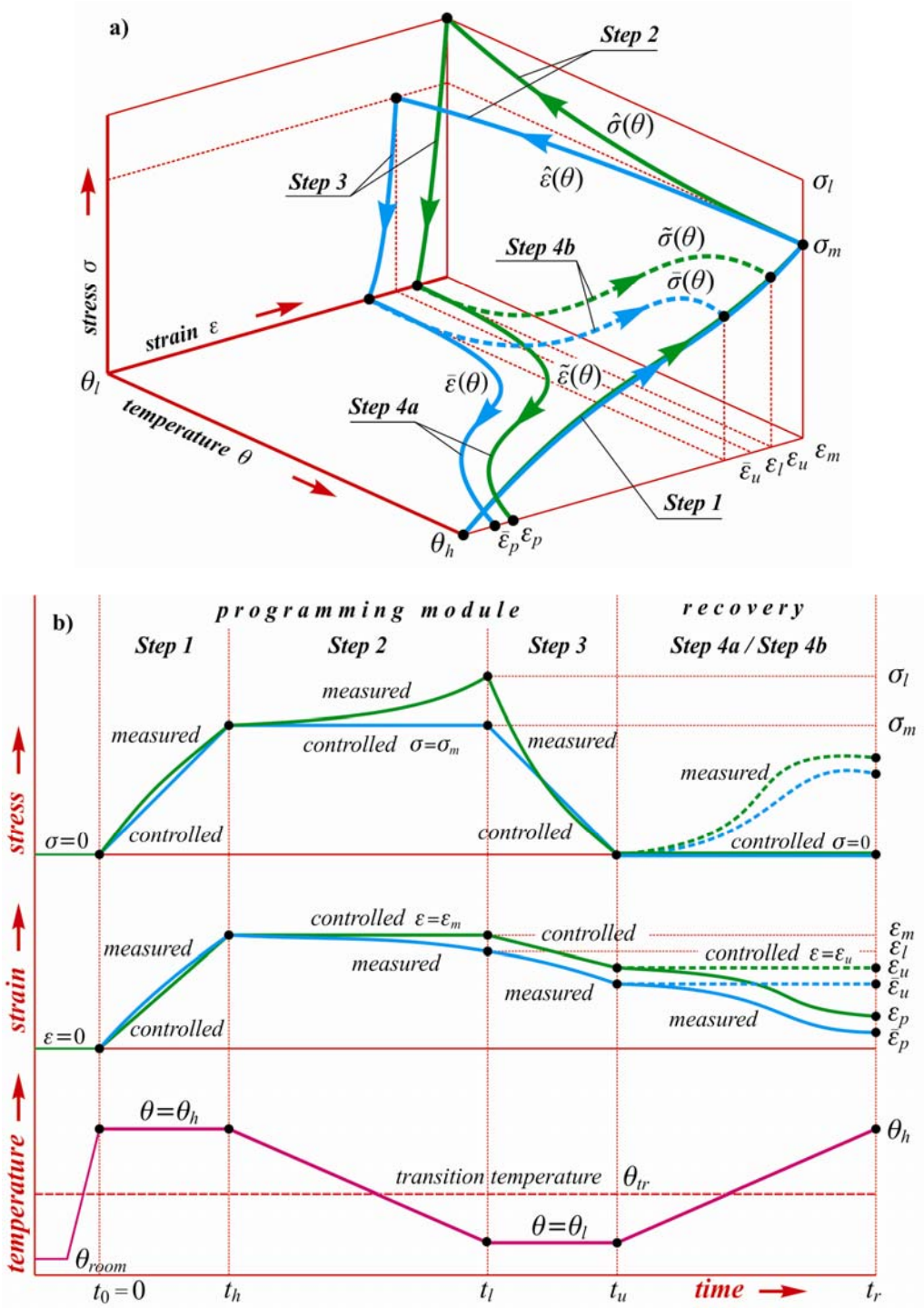

Fig. 1. One-way shape memory cycles represented as: a) single curve in 3D strain-stress-temperature space and b) corresponding three curves (temperature-time, strain-time, and stress-time) in the respective 2D spaces. Strain-controlled (green) and stress-controlled (blue) programming module followed by either unconstrained (solid lines) or constrained (interrupted lines) recovery process.

Shape Memory Effect (SME) in polymers is a result of structure, morphology, and processing of a material [2, 6, 11, 16]. At macroscale, this effect is conveniently demonstrated in multiple steps experiments known as thermomechanical shape memory cycles (SMCs), cf. Fig. 1. A detailed discussion of SMCs has been presented in [6, 9, 11 - 13]. First, a polymer is conventionally processed to achieve a desired permanent shape. Then, it is mechanically deformed and fixed in a temporary shape. This process is called programming and is done by heating up, deforming in the hot state, and cooling down the material to fix the temporary shape. To trigger the memory effect, the material is heated up again above the transformation temperature to recover its original permanent shape. Depending on the instrument used in the test, the programming process can be conducted either in strain- or stress-controlled mode and the recovery process can be performed in unconstrained or constrained mode. In effect, there are four basic types of SMCs, each consisting of four main steps. This is illustrated in Fig. 1 and described below. Here it should be added that a study of the influence of viscoelastic (time and rate) effects on the shape memory behavior of SMPs requires more general SMCs that include additional sub-steps (holding time) [11-13]. However, the thermoelastic constitutive models considered in this paper do not account for such effects and therefore the standard SMC suffices to test these models.

To start the standard uniaxial SMC shown in Fig. 1, a SMP's sample is brought to state at an elevated temperature $\theta_h > \theta_{tr}$ (which is above the transformation temperature θ_{tr}) at zero strain and stress ($\sigma = 0$, $\varepsilon = 0$). This state is considered as a permanent shape of the polymer and all subsequent strains and stresses are measured with respect to this state. Then the thermomechanical cycle in strain- or stress- controlled mode consists of four successive steps.

1. *High-temperature deformation:* Temperature is held fixed at the so-called deformation temperature (here assumed to coincide with the high temperature θ_h) and the sample is deformed to a pre-determined maximal strain ε_m (in strain-controlled mode) or stress σ_m (in stress-controlled mode).
2. *Cooling and fixing the temporary shape*: Under imposed strain or stress constraint, the sample is cooled from the deformation temperature $\theta_h > \theta_{tr}$ to a low (setting) temperature $\theta_l < \theta_{tr}$. The resulting strain and stress at θ_l are denoted by ε_l and σ_l, respectively.
   - *Strain-controlled mode*: Strain is kept at the pre-determined strain ε_m and the resulting stress $\sigma = \hat{\sigma}(\theta)$ is measured as a function of temperature (***Step 2 - green***).
   - *Stress-controlled mode:* Stress is kept at the pre-determined stress σ_m and the corresponding strain $\varepsilon = \hat{\varepsilon}(\theta)$ is measured as a function of temperature (***Step 2 - blue***).
3. *Low temperature unloading process*: At the low temperature θ_l, the strain (stress) constraint is released resulting in a spontaneous spring back of the sample and the stress reduces to zero, $\sigma = 0$. The corresponding strain at unloading, denoted by ε_u and $\bar{\varepsilon}_u$, respectively, is the amount of strain stored in the material (***Step 3 - green*** or ***Step 3 - blue***). In this state, the temporary shape of the sample is fixed.
4. *Recovery process:* The temporarily deformed sample is heated back to the high temperature θ_h above θ_{tr}. This process may be continued in one of two ways:
   - *Unconstrained recovery process:* Heating the material sample to the temperature θ_h without any strain constraint. In this case, the sample tries to recover the original shape displaying the shape memory effect (***Step 4a - green*** or ***Step 4a - blue***). If an irrecoverable deformation was imparted to the sample during the cycle, then the resulting strain is defined as ε_p and $\bar{\varepsilon}_p$, respectively, and the corresponding stress is zero for a non-constrained recovery step, $\sigma = 0$.

- *Constrained recovery process:* Heating the material sample to the temperature θ_h while holding the strain at ε_u or $\bar{\varepsilon}_u$, respectively. In this case, the material develops a stress recovery (***Step 4a - green*** or ***Step 4b - blue***).

In effect, the stress storage profile $\hat{\sigma}(\theta)$, the unconstrained strain recovery profile $\tilde{\varepsilon}(\theta)$ as well as the constrained stress recovery profile $\tilde{\sigma}(\theta)$ are measured in strain-controlled SMCs tests. In stress-controlled SMCs tests, the strain storage profile $\hat{\varepsilon}(\theta)$, the unconstrained strain recovery profile $\bar{\varepsilon}(\theta)$ as well as the constrained stress recovery profile $\bar{\sigma}(\theta)$ are measured.

The ability of a particular SMP to fix a temporary shape and to restore a permanent (original) shape are quantified by the shape fixity (also called the strain fixity ratio) R_f and the shape recovery (also called the strain recovery ratio) R_r, which are defined by [6, 11 - 13]

$$R_f = \frac{\varepsilon_u}{\varepsilon_m}, \qquad R_r = \frac{\varepsilon_m - \varepsilon_p}{\varepsilon_m} \tag{1}$$

for the strain-controlled SMC tests, and

$$R_f = \frac{\bar{\varepsilon}_u}{\varepsilon_l}, \qquad R_r = \frac{\varepsilon_l - \bar{\varepsilon}_p}{\varepsilon_l} \tag{2}$$

for the stress-controlled SMC tests. Here ε_m, ε_u, ε_p, and ε_l, $\bar{\varepsilon}_u$, $\bar{\varepsilon}_p$ are the strains measured in the corresponding SMCs (Fig. 1). The quantitative analysis of both the shape fixity and recovery is a major concern in the development of shape memory polymers for specific applications. However, for the formulation of constitutive models of SMPs and for the calibration of the respective material parameters it is necessary to measure the complete strain/stress storage/recovery profiles for different values of pre-strain ε_m (or pre-stress σ_m) besides the stress-strain relations at high and lower temperature.

3. Linear thermoelastic model

A detailed discussion of various constitutive theories belonging to the class of linear thermoelastic (LTE) models is given in [14] and further details may be found in the original papers [6, 16, 18 - 27]. Here we present the mathematical generalization of all these models.

Any constitutive theory for thermally-responsive SMPs must relate the strain history $\varepsilon(t)$, stress history $\sigma(t)$, and temperature history $\theta(t)$ for any time interval $[t_0, +\infty)$. Here ε and σ are the uniaxial strain and the work-conjugate stress, respectively. Moreover, t_0 denotes the initial time instant at which the tested shape memory polymer is in the stress and strain free state at reference temperature θ_0. Thus, the strain, stress, and temperature histories satisfy the following initial conditions

$$\varepsilon(t_0) = 0, \qquad \sigma(t_0) = 0, \qquad \theta(t_0) = \theta_0. \tag{3}$$

The formulation of the linear thermoelastic (LTE) theory for SMPs is based on the assumption that the total strain $\varepsilon(t)$ at any time t may be decomposed additively (see Liu et al. [18, 19]),

$$\varepsilon(t) = \varepsilon_e(t) + \varepsilon_\theta(t) + \varepsilon_s(t), \tag{4}$$

into the sum of the mechanical (elastic) strain $\varepsilon_e(t)$, the thermal strain $\varepsilon_\theta(t)$, and the so-called stored or frozen strain $\varepsilon_s(t)$. It is further assumed that partial strains at any time instant t are specified by the following general constitutive laws:

- the mechanical (elastic) strain depends on the current stress and temperature only and is linear with respect to stress

$$\varepsilon_e(t) = C(\theta(t))\sigma(t), \tag{5}$$

- the thermal strain depends on the temperature history only

$$\varepsilon_\theta(t) = \int_{t_0}^{t} \alpha_\theta(\theta(\tau))\dot{\theta}(\tau)d\tau, \tag{6}$$

- the stored strain depends on the stress and temperature histories

$$\varepsilon_s(t) = \int_{t_0}^{t} D(\theta(\tau))\sigma(\tau)\dot{\theta}(\tau)d\tau. \tag{7}$$

In these constitutive laws, the superimposed dot stands for the derivative with respect to time and $\tau \in [t_0, t]$ is the running integration time.

The simplicity of the LTE theory for shape memory polymers lies in the fact that the constitutive relations reduce to a single law of the following general form

$$\varepsilon(t) = C(\theta(t))\sigma(t) + \int_{t_0}^{t} \alpha_\theta(\theta(\tau))\dot{\theta}(\tau)d\tau + \int_{t_0}^{t} D(\theta(\tau))\sigma(\tau)\dot{\theta}(\tau)d\tau. \tag{8}$$

This law gives the total strain $\varepsilon(t)$ at any time t in terms of stress and temperature histories, $\sigma(\tau)$ and $\theta(\tau)$, $\tau \in [t_0, t]$, satisfying the initial conditions (3). The general constitutive theory for the LTE models involves three response functions each being a function of temperature only:

$\alpha_\theta(\theta)$ – the coefficient of overall thermal expansion,
$C(\theta)$ – the instant elastic compliance, and
$D(\theta)$ – the so-called distributed elastic compliance.

From a practical point of view, it suffices to determine these response functions in an experimental program. Various special theories in the class of LTE models differ in the forms these response functions are assumed.

4. Two-phase LTE models

Thermally-responsive SMPs basically consist of two phases, the frozen (rigid) and the thermally reversible (mobile) phase [2, 4, 13]. The thermally reversible phase is generally designed to have a large drop in elastic modulus on heating through the transformation temperature θ_{tr} (the glass transition temperature θ_g of an amorphous phase or the melting temperature θ_m of a crystalline phase). These fundamental observations schematically shown in Fig. 2 provide the physical basis for macroscopic (phenomenological) constitutive LTE models considering SMPs as a two-phase material. Within this concept, the shape memory effect in polymers is considered as a result of two concurrent processes:

a) the transition from rubbery behavior dominated by entropic energy at high temperatures (above the transition temperature, either θ_g or θ_m) to glassy or semicrystalline behavior dominated by internal energy at low temperatures (below the transition temperature) and
b) the storage of the deformation incurred at high temperatures during cooling.

In the mathematical modeling, these physical mechanisms are accounted for through two state variables:

a') the frozen fraction function φ describing the volume fraction of the frozen (glassy or semicrystalline) phase, and

b') the stored or frozen strain ε_s describing the strain that is stored (memorized) in the material during freezing.

In Liu et al. [18, 19], the shape memory polymer is described as a composite material where two phases coexist in the temperature range that defines the glass transition with volume fractions, which depend on temperature only. The glassy or "frozen" phase with a volume fraction $\varphi(\theta)$ has the elastic behavior, which stems from internal energy, whereas the elastic behavior of the rubbery or "active" phase with a volume fraction $1-\varphi(\theta)$ originates essentially from the entropy of macromolecular chains. In the cooling step (Step 2 in SMC, see Fig. 1), the glass transition develops from a high temperature θ_h, where (and above which) $\varphi(\theta)=0$, to a low temperature θ_l, where (and below which) $\varphi(\theta)=1$. Discussion of various special forms of $\varphi(\theta)$ proposed in the literature has been presented in [31].

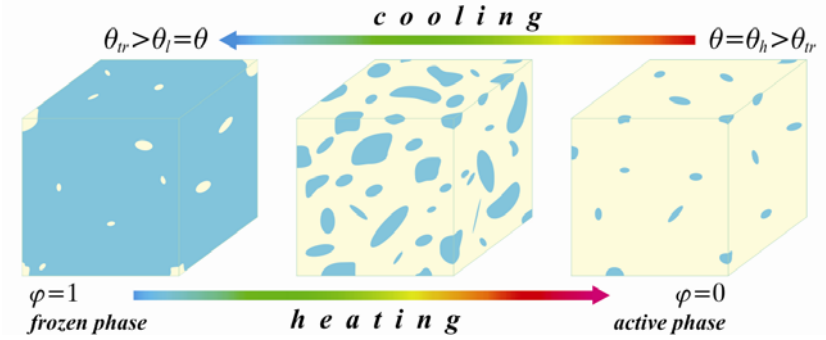

Fig. 2. Two phase model of the shape memory behavior of polymers

All LTE models generalizing the original formulation of Liu et al. [18, 19] are based on the temperature-dependent frozen volume fraction $\varphi(\theta)$, which is used for evaluation the overall elastic behavior of two-phase SMPs defining their overall thermal expansion and describing the shape memory effect. In general case, the coefficient of overall thermal expansion $\alpha_\theta(\theta)$ is assumed in the form derived from a simple mixture rule

$$\alpha_\theta(\theta)=\varphi(\theta)\alpha_\theta^g(\theta)+(1-\varphi(\theta))\alpha_\theta^r(\theta)\,. \tag{9}$$

The response functions $C(\theta)$ and $D(\theta)$, the instant elastic compliance and the distributed elastic compliance, are given by (Reuss average)

$$C(\theta)=\frac{\varphi(\theta)}{E_g(\theta)}+\frac{1-\varphi(\theta)}{E_r(\theta)} \tag{10}$$

and (incremental Reuss average)

$$D(\theta)=-\left\{\frac{1}{E_g(\theta)}-\frac{1}{E_r(\theta)}\right\}\frac{d\varphi(\theta)}{d\theta}\,, \tag{11}$$

respectively. The LTE models described by the general constitutive law (8) with response functions $\alpha_\theta(\theta)$, $C(\theta)$ and $D(\theta)$ defined by (9) - (11), respectively, require the calibration of five response functions:

- the coefficients of thermal expansion $\alpha_\theta^g(\theta)$ and $\alpha_\theta^r(\theta)$ in the glassy (frozen) and rubbery (active) phase of a particular SMP,
- the elastic moduli $E_g(\theta)$ and $E_r(\theta)$ for these two phases, and
- the frozen volume fraction function $\varphi(\theta)$.

Different specific forms of these response functions determine a particular constitutive theory in the broad class of LTE models.

In general, the three response functions $E_g(\theta)$, $E_r(\theta)$ and $\varphi(\theta)$ appear in the constitutive relations (10) and (11) only through the functions $C(\theta)$ and $D(\theta)$. It then follows that the polymer behavior under uniaxial tension is completely described by the three response functions, $\alpha_\theta(\theta)$, $C(\theta)$ and $D(\theta)$. Thus, it suffices to determine these response functions in an appropriate experimental program.

The general constitutive law (8) with the response functions $\alpha_\theta(\theta)$, $C(\theta)$ and $D(\theta)$ defined by (9) - (11) was first derived by Chen et al. [20] as generalization of the original formulation proposed by Liu et al. [18, 19]. In recent work by Gilormini and Diani [14], the more general forms than (9) - (11) for $\alpha_\theta(\theta)$, $C(\theta)$ and $D(\theta)$ have been derived by applying different mixture rules. This generalization and many other possible ones are included in the formulation presented in Section 3.

5. Special two-phase LTE models

The constitutive relations of the original Liu et al. two-phase model [18, 19] follow from (9) - (11) under the additional assumptions that $E_r(\theta)$ is linear in temperature θ, $E_g(\theta)$ is independent of θ, and $E_g(\theta)$ is absent in the definition of the distributed compliance $D(\theta)$:

$$C(\theta) = \frac{\varphi(\theta)}{E_G} + \frac{1-\varphi(\theta)}{(\theta/\theta_h)E_R}, \qquad D(\theta) = \frac{1}{(\theta/\theta_h)E_R}\frac{d\varphi(\theta)}{d\theta}. \tag{12}$$

Here E_G and E_R are constant elastic moduli for the glassy and rubbery phase, respectively. In addition, Liu et al. [18, 19] assumed the frozen function in a specific (empirical) form

$$\varphi = \hat{\varphi}(\theta) \equiv 1 - \frac{1}{1 + c_f(\theta_h - \theta)^n}, \tag{13}$$

where θ_h is the pre-deformation temperature, c_f and n are model parameters, which must be determined by data. The parameter n is dimensionless and the physical unit of the parameter c_f is $1/\mathrm{K}$. Moreover, the material constants were determined through curve fitting by using the strain recovery data without making use of the stress storage and recovery data. Nevertheless, the prediction of the model developed by Liu et al. [18, 19] agrees considerable with data measured by these authors for all three profiles (Fig. 3 and Fig. 4).

Chen et al. [20] observed that not all five response functions appearing in the Liu et al. model (9)-(11) are independent and three combinations of these functions suffice to specify the model. A possible choice of such combinations is given by the three response functions, for the thermal strain $\hat{\varepsilon}_\theta(\theta)$, the instant elastic compliance $C(\theta)$, and the distributed elastic compliance $D(\theta)$, as presented in the general two-phase model based on the constitutive relations (9) - (11). Chen et al. [20] presented also a different methodology to calibrate these response functions by using the experimental data obtained by Liu et al. [18, 19]. Furthermore, they have shown that it is possible to

use their approach to assess the applicability of the assumptions made in [18, 19]. Theoretical solutions presented in Chen et al. [20] coincide very well with the data of [18, 19] for the stress storage and strain recovery profiles. However, it is rather unexpected to see that the theoretical results for the stress recovery profiles obtained by Chen et al. [20] are actually less accurate than the solutions given in [18, 19] (see Fig. 4). Chen et al. [20] noted that this discrepancy might be due to measurement errors or inaccuracy of the model.

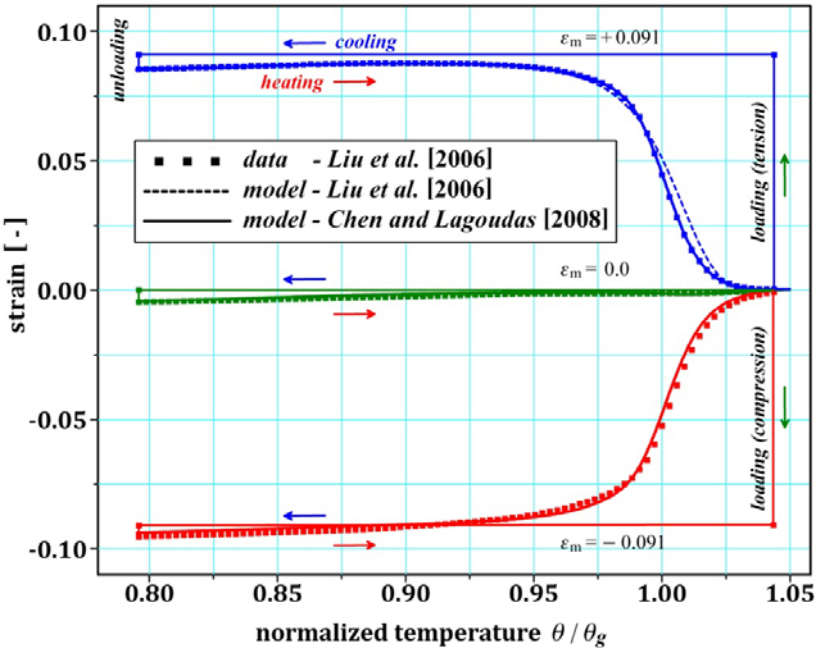

Fig. 3. Unconstrained strain recovery for different pre-strains: Comparison of data and model prediction presented by Liu at al. [19].

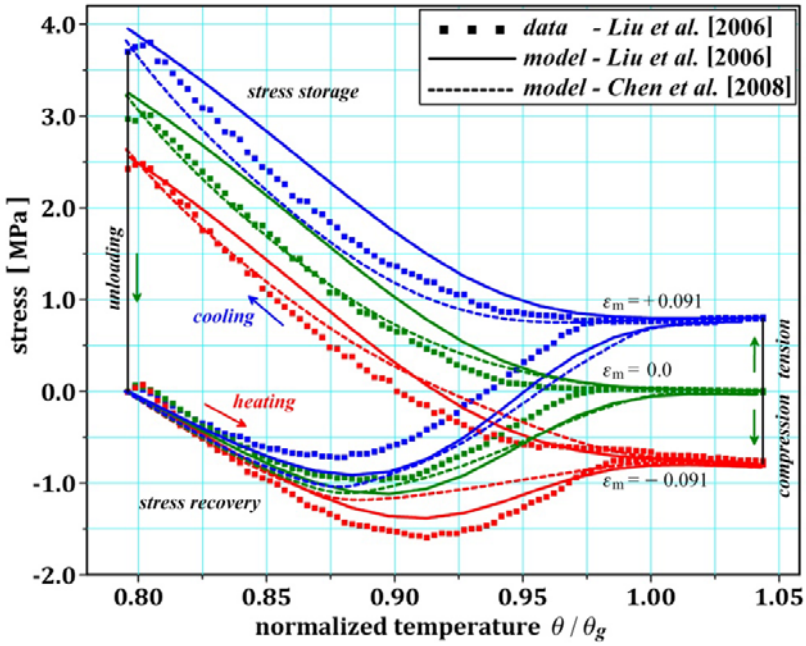

Fig. 4. Stress storage and recovery profiles for different pre-strains: Comparison of data (Liu at al. [19]) and model prediction (Liu at al. [19] and Chen et al. [20]).

The approach of Chen et al. [20] have been followed by Volk [16]. He assumed that both moduli, $E_g(\theta)$ and $E_r(\theta)$, are independent of temperature. In effect, the response functions $C(\theta)$ and $D(\theta)$ in his formulation take the forms

$$C(\theta) = \frac{1-\varphi(\theta)}{E_R} + \frac{\varphi(\theta)}{E_G}, \qquad D(\theta) = \left\{\frac{1}{E_R} - \frac{1}{E_G}\right\}\frac{d\varphi(\theta)}{d\theta}, \tag{14}$$

where E_G and E_R are the elastic moduli for the glassy and rubbery phases, respectively. It is interesting to note that in this special case

$$\frac{dC(\theta)}{d\theta} = -D(\theta), \tag{15}$$

as may be easily verified by taking time derivative of $(14)_1$. Experimental investigations by Volk [20] lack the capability to directly measure the frozen volume fraction during the experiment. As a result, the frozen volume fraction was assumed to take a shape similar to that of the shape recovery profile upon heating at zero load. Consequently, a hyperbolic tangent function is assumed for the frozen volume fraction and optimized to fit the strain recovery profile, which is used for calibration. Volk [20] tested his model against its own data but no comparison with Liu et al. model and data has been presented.

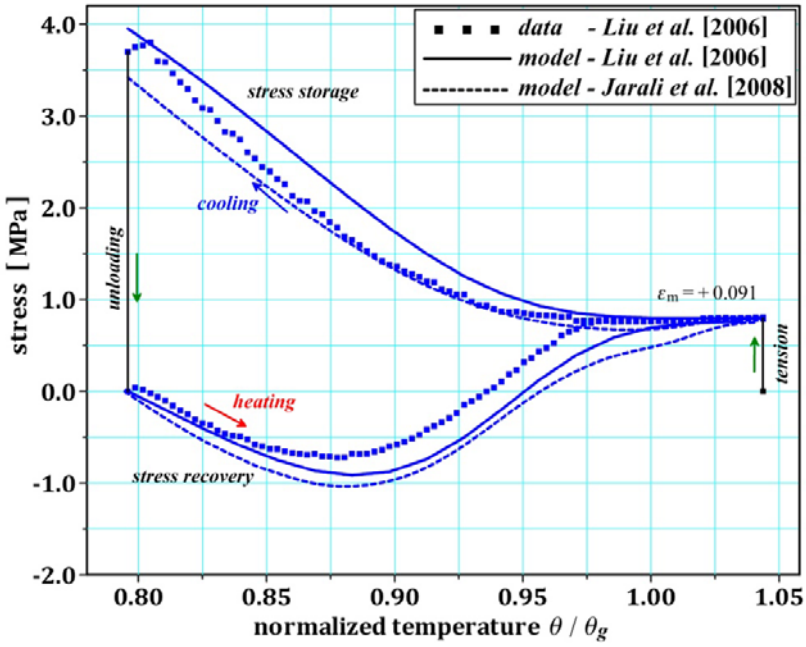

Fig. 5. Constrained stress recovery profiles for different pre-strains: Comparison of data (Liu at al. [19]) and model prediction (Liu at al. [19] and Jarali et al. [22, 25]).

Many other authors made numerous attempts to improve the original Liu et al. model and to extend its range of applicability. In particular, in [22] and [25], a more general constitutive law for the thermal strain was proposed while keeping the remaining constitutive relations in the original Liu et al. form. This modification gives a slightly better prediction of the stress storage profile but not of the stress recovery profile than the original model (Fig. 5).

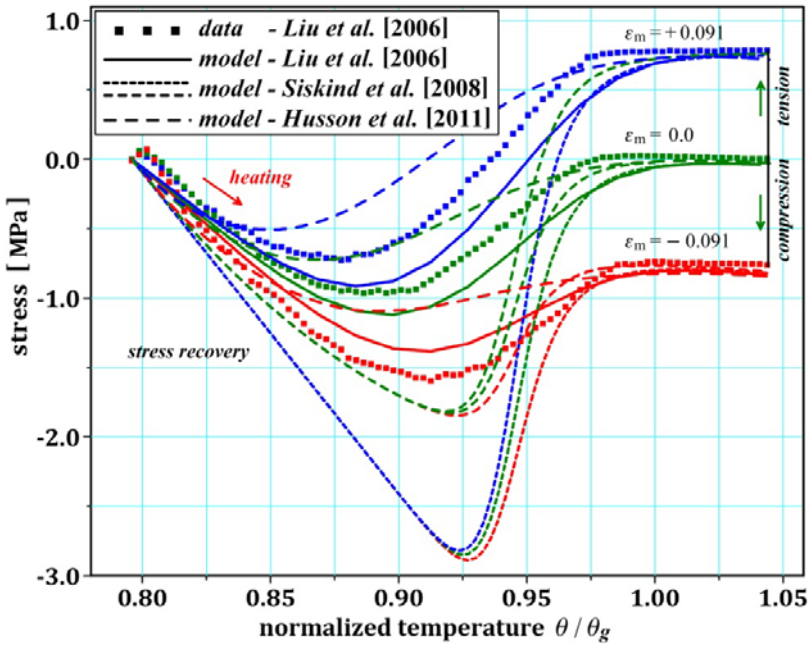

Fig. 6. Constrained stress recovery profiles for different pre-strains: Comparison of data (Liu at al. [19]) and model prediction (Liu at al. [19], Siskind et al. [26, 27] and Husson et al. [24]).

In Husson et al. [24], the thermal strains measured by Liu et al. [19] have been interpolated using a third degree polynomial keeping the remaining constitutive equations in form derived by Liu et al. The obtained with this slight modifications solutions give somewhat better coincidence of the results with data for the stress storage but less accurate for the stress recovery (Fig. 6). Still another attempt to improve the Liu et al. model has been presented in Siskin et al. [26, 27]. However, the two versions of their model tested against the Liu et al. data give rather poor predictions of the stress recovery profiles (Fig. 6).

At the microscale, the original Liu et al. model and its various generalizations proposed in the literature may be considered as a two-phase composite with glassy and rubbery phases having volume fractions that depend on temperature only. In addition, a uniform stress hypothesis was used in the original formulation with an inconsistency when the thermal expansion was considered. In a very recent paper by Gilormini and Diani [14], Liu's et al. model is revisited by taking advantage of the results that have been established in theories of composite materials (Fig. 7). As in the original Liu formulation, they considered the SMP as a composite material, where two phases coexist in temperature range that define the glass transition, with volume fractions that depend on temperature only. However, they argued that a uniform strain hypothesis is more appropriate than assuming a uniform stress as in Liu et al.

Summarizing this analysis, it should be noted that actually none of the "improved" or "extended" models proposed in the literature gives a better prediction than the original model due to Liu et al. The suggestion by Chen et al. [20] that the failure of their model may be due to measurement errors or inaccuracy of the model also does not explain this rather unexpected and certainly undesired fact. This simply means that a more reliable methodology is required for the evaluation of the LTE models.

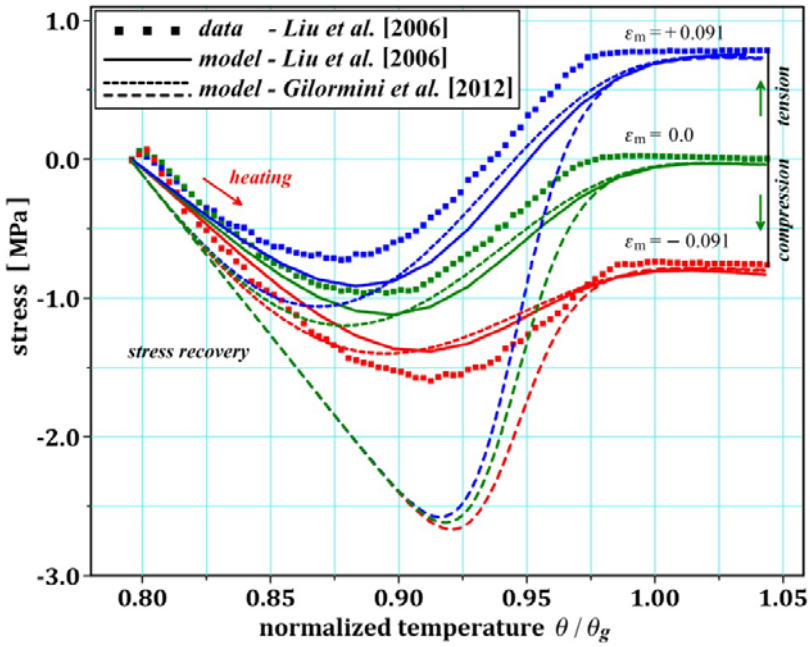

Fig. 7. Constrained stress recovery profiles for different pre-strains: Comparison of data (Liu at al. [19]) and model prediction (Liu at al. [19] and Gilormini et al. [14]).

6. Simulation of shape memory cycles

Given the relevant response functions, various special LTE models discussed in the previous Sections may be used for the analysis of the shape memory behavior of polymers, in general, and for the simulation of SMCs in both strain- and stress controlled mode, in particular. In this section, we specify the LTE constitutive law for successive steps of SMCs largely following the approach first proposed by Chen et al. [20] and subsequently used by Volk [16] and Li [21]. Our analysis is more general in that we do not use the particular constitutive relations (9) - (11) for the special two-phase models but instead we directly base our considerations on the general law (8) with $\alpha_\theta(\theta)$, $C(\theta)$ and $D(\theta)$ as the basic response functions of any possible form.

6.1 Strain-controlled SMCs

The constitutive law (8) relates the strain history $\varepsilon(t)$, the stress history $\sigma(t)$, and the temperature history $\theta(t)$ and serves for determination of any one from given two others. In particular, when specified for successive steps of the strain-controlled SMCs described in Section 2 (Fig. 1, green curves), this general constitutive law assumes the following specials forms.

Step 1. Mechanical loading of a sample at constant temperature $\theta(t) = \theta_h$, $\theta_h \geq \theta_{tr}$, implies that the thermal and storage strains are both zero, i.e. $\varepsilon_\theta(t) = \varepsilon_s(t) = 0$ in the time interval $[t_0, t_h]$, Fig. 1. In effect, the constitutive law (8) reduces to Hooke's law

$$\varepsilon(t) = C(\theta_h)\sigma(t), \qquad t_0 \leq t \leq t_h, \tag{16}$$

where $C(\theta_h)$ is the elastic compliance computed at high temperature θ_h.

Step 2. The temperature and strain history for the second step of the strain-controlled SMC are $\theta(t)=\hat{\theta}(t)$ and $\varepsilon(t)=\varepsilon_m$ in the time interval $[t_h,t_l]$. Here $\hat{\theta}(t)$ is the prescribed temperature evolution during cooling from high to low temperature usually assumed in ramp form $\hat{\theta}(t)=\theta_h+\beta_c(t-t_h)$, where $\beta_c<0$ denotes the cooling rate. Then the constitutive law (8) for the second step of SMC takes the form

$$\varepsilon_m=C(\theta(t))\sigma(t)+\int_{t_h}^{t}\alpha_\theta(\theta(\tau))\dot{\theta}(\tau)d\tau+\int_{t_h}^{t}D(\theta(\tau))\sigma(\tau)\dot{\theta}(\tau)d\tau\,,\qquad t_h\le t\le t_l\,. \tag{17}$$

Since the temperature is constant in the first time interval $[t_0,t_h]$, the low integration limit t_0 in (17) has been replaced by the initial time t_h of the second step. Assuming that the temperature history $\hat{\theta}(t)$ is a monotone decreasing function of time with $\theta_h=\theta(t_h)$, the constitutive law (17) may be reformulated with respect to temperature as the independent variable

$$\varepsilon_m=C(\theta)\hat{\sigma}(\theta)+\int_{\theta_h}^{\theta}\alpha_\theta(\zeta)d\zeta+\int_{\theta_h}^{\theta}D(\zeta)\hat{\sigma}(\zeta)d\zeta\,,\qquad \theta_h\ge\theta\ge\theta_l\,. \tag{18}$$

Here ζ denotes the running temperature in the integration interval and $\hat{\sigma}(\theta)$ is a function of temperature such that $\sigma(t)=\hat{\sigma}(\theta(t))$ during the second step of SMC.

Step 3. At the end of the second step, the temperature reaches the low temperature θ_l and the third step of SMC consists of unloading the sample while the temperature is held fixed at low temperature, i.e. $\theta(t)=\theta_l$ so that $\dot{\theta}(t)=0$ in time interval $[t_l,t_u]$. By implication, the general law (8) reduces to the linear (actually, affine) form

$$\varepsilon(t)=C(\theta_l)\sigma(t)+\hat{\varepsilon}_\theta(\theta_l)+\hat{\varepsilon}_s(\theta_l)\,,\qquad t_l\le t\le t_u\,, \tag{19}$$

where $C_l=C(\theta_l)$ is the elastic compliance evaluated in the glassy phase and

$$\begin{aligned}\hat{\varepsilon}_\theta(\theta_l)&=\int_{t_h}^{t_l}\alpha_\theta(\theta(t))\dot{\theta}(\tau)d\tau=\int_{\theta_h}^{\theta_l}\alpha_\theta(\theta)d\theta\,,\\ \hat{\varepsilon}_s(\theta_l)&=\int_{t_h}^{t_l}D(\theta(\tau))\sigma(\tau)\dot{\theta}(\tau)d\tau=\int_{\theta_h}^{\theta_l}D(\theta)\hat{\sigma}(\theta)d\theta\end{aligned} \tag{20}$$

are thermal and storage strains accumulated during the second step. These strains are constant in the third step of SMC.

The fourth and last step of SMC involves heating of the sample either under stress free condition or at fixed strain.

Step 4a. During the unconstrained shape recovery at stress free condition, the temperature and stress history are given by $\theta(t)=\tilde{\theta}(t)$ and $\sigma(t)=0$ for the time interval $[t_u,t_r]$. Here $\tilde{\theta}(t)$ is a function describing variation of temperature during heating. In ramp form, it reads $\tilde{\theta}(t)=\theta_l+\beta_h(t-t_l)$, where $\beta_h>0$ is the heating rate. In effect, the constitutive law (8) takes the form

$$\varepsilon(t)=\int_{t_h}^{t}\alpha_\theta(\theta(\tau))\dot{\theta}(\tau)d\tau+\int_{t_h}^{t}D(\theta(\tau))\sigma(\tau)\dot{\theta}(\tau)d\tau\,,\qquad t_u\le t\le t_r\,. \tag{21}$$

Let us note that the temperature is constant in the sub-intervals $[t_0,t_h]$ and $[t_l,t_u]$, and hence the integrals in (21) over these interval are zero. Moreover, with the strain function $\tilde{\varepsilon}(\theta)$ defined by $\varepsilon(t)=\tilde{\varepsilon}(\theta(t))$ and the use of the stress profile $\sigma(t)=\hat{\sigma}(\theta(t))$ determined in the second step of SMC makes it possible to reformulate the constitutive relation (21) as

$$\tilde{\varepsilon}(\theta) = \int_{\theta_h}^{\theta} \alpha_\theta(\zeta) d\zeta + \int_{\theta_h}^{\theta} D(\zeta)\hat{\sigma}(\zeta) d\zeta \,, \qquad \theta_l \le \theta \le \theta_h \,. \tag{22}$$

The constitutive relation (22) serves to determine the unconstrained strain recovery profile $\tilde{\varepsilon}(\theta)$ for given temperature history at zero stress state. On the other hand, $\tilde{\varepsilon}(\theta)$ is a function of temperature representing the unconstrained strain recovery profiles and thus it is an experimentally measurable function.

Step 4b. The last step of SMC may alternatively be carried out at fixed strain. In this case, instead of heating at zero stress, the specimen is heated at the constant strain ε_u that has occurred at the end of unloading $\theta(t) = \tilde{\theta}(t)$ and $\varepsilon(t) = \varepsilon_u$ in the time interval $[t_u, t_r]$. The general constitutive law (8) takes the form

$$\varepsilon_u = C(\theta(t))\sigma(t) + \int_{t_0}^{t} \alpha_\theta(\theta(\tau))\dot{\theta}(\tau) d\tau + \int_{t_0}^{t} D(\theta(\tau))\sigma(\tau)\dot{\theta}(\tau) d\tau \,, \qquad t_u \le t \le t_r \,, \tag{23}$$

and serves for the stress determination during this step. The integral terms in (23) determine the thermal strain and the accumulated storage strain, respectively, at any time t in the interval $[t_u, t_r]$. Denoting by $\tilde{\sigma}(\theta)$ the stress as a function of temperature during heating and by $\hat{\sigma}(\theta)$ the stress as a function of temperature during initial cooling leads to the following constitutive equation

$$\varepsilon_u = C(\theta)\tilde{\sigma}(\theta) + \hat{\varepsilon}_\theta(\theta) + \int_{\theta_h}^{\theta} D(\zeta)\hat{\sigma}(\zeta) d\zeta \,, \qquad \theta_l \le \theta \le \theta_h \,, \tag{24}$$

where the integral term determines the stored strain at any temperature in temperature interval during heating. If the response functions $\hat{\varepsilon}_\theta(\theta)$, $C(\theta)$ and $D(\theta)$ are given, and the function $\hat{\sigma}(\theta)$ is known from the solution of the second step, then the constitutive relation (24) can be solved for $\tilde{\sigma}(\theta)$.

The constitutive relations (16), (18), (19), (22) and (24) for the successive steps of the strain-controlled SMCs have been previously derived by Chen et al. [20] with $\alpha_\theta(\theta)$, $C(\theta)$ and $D(\theta)$ given by relations (9) - (11) for the two-phase LTE model (see also Volk [16] for some special cases). The considerations above show that these a priori assumptions need not be introduced at this stage of the analysis and the constitutive relations derived above apply for the response functions $\alpha_\theta(\theta)$, $C(\theta)$ and $D(\theta)$ of any form.

6.2 Stress-controlled SMCs

By the same arguments as in the preceding sub-section, the general constitutive law (8) may be specified for all steps of the stress-controlled SMCs (Fig. 1, blue curves).

Step 1. A sample from the reference (strain and stress free) state to a prescribed stress $\sigma = \sigma_m$ is carried out at the fixed temperature θ_h, so that $\theta(t) = \theta_h$, and the constitutive law (8) reduces again to the linear form (16).

Step 2. The second step of SMC involves cooling of the sample with the stress held at fixed value σ_m attained at the end of the first step. Accordingly, $\theta = \theta(t)$ and $\sigma(t) = \sigma_m$ in the time interval $[t_h, t_l]$ and the constitutive law (8) reduces to the form

$$\varepsilon(t) = \hat{\varepsilon}_\theta(\theta(t)) + \left(C(\theta(t)) + \int_{t_0}^{t} D(\theta(\tau))\dot{\theta}(\tau) d\tau \right) \sigma_m \,, \qquad t_h \le t \le t_l \,. \tag{25}$$

During this step, the temperature is a monotone decreasing function of time and the constitutive law (25) may be reformulated again with respect to temperature

$$\hat{\varepsilon}(\theta) = \hat{\varepsilon}_\theta(\theta) + \left(C(\theta) + \int_{\theta_h}^{\theta} D(\zeta) d\zeta \right) \sigma_m , \qquad \theta_h \geq \theta \geq \theta_l , \tag{26}$$

where $\hat{\varepsilon}(\theta)$ is defined by $\varepsilon(t) = \hat{\varepsilon}(\theta(t))$. It follows that for a given maximum stress σ_m, the constitutive equation (26) serves to determine the strain history $\hat{\varepsilon}(\theta)$ for any given temperature evolution $\theta = \theta(t)$.

On the other hand, the function $\hat{\varepsilon}(\theta)$ represents the strain profile during the cooling process and hence it is an experimentally measurable function. This process ends when a temperature reaches the so-called low temperature $\theta = \theta_l$ with the corresponding strain $\varepsilon_l = \hat{\varepsilon}(\theta_l)$, which is also a measured quantity called the frozen strain.

Step 3. Unloading at low temperature, i.e. $\theta(t) = \theta_l$ in the time interval $[t_l, t_u]$, yields the constitutive law in the linear (affine form)

$$\varepsilon(t) = C(\theta_l)\sigma(t) + \hat{\varepsilon}_\theta(\theta_l) + \hat{\varepsilon}_s(\theta_l) \tag{27}$$

with the accumulated thermal and storage strain given by

$$\hat{\varepsilon}_\theta(\theta_l) = \int_{\theta_h}^{\theta_l} \alpha_\theta(\theta) d\theta , \qquad \hat{\varepsilon}_s(\theta_l) = \int_{\theta_h}^{\theta_l} D(\theta)\sigma(\theta) d\theta . \tag{28}$$

Step 4a. Heating of the sample under stress free conditions is determined by the temperature and stress history $\theta = \tilde{\theta}(t)$ and $\sigma(t) = 0$ in the time interval $[t_l, t_r]$. The constitutive law (8) takes to the form

$$\varepsilon(t) = \hat{\varepsilon}_\theta(\theta(t)) + \int_0^t D(\theta(\tau))\sigma(\tau)\dot{\theta}(\tau) d\tau . \tag{29}$$

With the strain function $\bar{\varepsilon}(\theta)$ defined by $\varepsilon(t) = \bar{\varepsilon}(\theta(t))$, the use of the constant stress σ_m in the second step of SMC makes it possible to write the constitutive relation (29) as

$$\bar{\varepsilon}(\theta) = \hat{\varepsilon}_\theta(\theta) + \left(\int_{\theta_h}^{\theta} D(\zeta) d\zeta \right) \sigma_m . \tag{30}$$

Given the response functions $\hat{\varepsilon}_\theta(\theta)$ and $D(\theta)$, the constitutive equation (30) serves to determine the strain history $\varepsilon(t) = \bar{\varepsilon}(\theta(t))$ for any given $\theta = \theta(t)$. On the other hand, the function of temperature $\bar{\varepsilon}(\theta)$ represents the unconstrained strain recovery profile and thus it is an experimentally measurable function.

Step 4b. Heating of the sample at fixed strain $\bar{\varepsilon}_u$, which has occurred at the end of unloading, is specified by $\theta = \theta(t)$ and $\varepsilon(t) = \bar{\varepsilon}_u$ in the time interval $[t_l, t_r]$ and the constitutive law (8) takes the form

$$\bar{\varepsilon}_u = C(\theta(t))\sigma(t) + \hat{\varepsilon}_\theta(\theta(t)) + \int_0^t D(\theta(\tau))\sigma(\tau)\dot{\theta}(\tau) d\tau . \tag{31}$$

Denoting by $\sigma(t) = \bar{\sigma}(\theta(t))$ the stress as a function of temperature during heating, the constitutive equations for this step reads

$$\bar{\varepsilon}_u = \hat{\varepsilon}_\theta(\theta) + C(\theta)\bar{\sigma}(\theta) + \left(\int_{\theta_h}^{\theta} D(\zeta) d\zeta \right) \sigma_m . \tag{32}$$

If the response functions $\varepsilon_\theta(\theta)$, $C(\theta)$ and $D(\theta)$ are given, the constitutive relation (32) can be solved for the function $\bar{\sigma}(\theta)$, which represents the stress recovery profile during heating and thus it is also an experimentally measurable function.

The derived constitutive relations (18), (19), (22) and (24) for the strain-controlled and (26), (28), (30) and (32) for the stress-controlled SMCs may now be used in various ways. If the involved response functions $\varepsilon_\theta(\theta)$, $C(\theta)$ and $D(\theta)$ are known or assumed, these relations may be used for the computation of all profiles in the respective SMCs and compared with data measured in the same cycles. The theoretical results presented in Section 5 were obtained in this way for various special constitutive relations and material parameters given in the relevant literature. Alternatively, the relations derived above may be used for the calibration of the relevant response functions appearing in the general constitutive law (8).

7. Calibration of the response functions

Noting that the constitutive relations (18) and (22) derived for Step 2 and Step 4a of the strain-controlled SMC involve the same terms for the thermal and storage strain, they may be simultaneously reduced to the form

$$C(\theta)\hat{\sigma}(\theta) = \varepsilon_m - \tilde{\varepsilon}(\theta), \qquad D(\theta)\hat{\sigma}(\theta) = \frac{d\tilde{\varepsilon}(\theta)}{d\theta} - \alpha_\theta(\theta). \tag{33}$$

These two relations contain the response functions $\alpha_\theta(\theta)$, $C(\theta)$ and $D(\theta)$ of the general LTE model, and the strain and stress profile, $\tilde{\varepsilon}(\theta)$ and $\hat{\sigma}(\theta)$, measured in the corresponding steps of SMC. The coefficient of thermal expansion $\alpha_\theta(\theta)$ for any polymeric material may be determined from standard thermal tests [15, 16, 19] such as Thermomechanical Analysis (TMA). It then follows that the instant elastic compliance $C(\theta)$ and the distributed elastic compliance $D(\theta)$ may be determined from the stress storage $\hat{\sigma}(\theta)$ and strain recovery $\tilde{\varepsilon}(\theta)$ profiles measured in Step 2 and Step 4a of the strain-controlled SMC.

In the same way, the relations (18) and (24) for Step 2 and Step 4b of the strain-controlled SMC may be reduced to the form

$$C(\theta)(\hat{\sigma}(\theta) - \tilde{\sigma}(\theta)) = \varepsilon_m - \varepsilon_u, \qquad D(\theta)\hat{\sigma}(\theta) = -\frac{d}{d\theta}\big(C(\theta)\tilde{\sigma}(\theta)\big) - \alpha_\theta(\theta). \tag{34}$$

Using these two relations, the response functions $C(\theta)$ and $D(\theta)$ may be determined directly from the stress storage $\hat{\sigma}(\theta)$ and stress recovery $\tilde{\sigma}(\theta)$ profile measured in the strain-controlled SMC provided that $\alpha_\theta(\theta)$ has been determined from the independent test.

The other important relation may be derived from the expressions $(33)_2$ and $(34)_2$ for the distributed elastic compliance $D(\theta)$, resulting in

$$\frac{d\tilde{\varepsilon}(\theta)}{d\theta} = -\frac{d}{d\theta}\big(C(\theta)\tilde{\sigma}(\theta)\big). \tag{35}$$

The integration of (35) in temperature sub-interval $[\theta_l,\theta] \subset [\theta_l,\theta_h]$ corresponding to the fourth step of the strain-controlled SMCs and taking into account that $\tilde{\varepsilon}(\theta_l) = \varepsilon_u$ and $\tilde{\sigma}(\theta_l) = 0$, one gets

$$C(\theta)\tilde{\sigma}(\theta) = \varepsilon_u - \tilde{\varepsilon}(\theta). \tag{36}$$

This gives another equation for the instant elastic compliance function $C(\theta)$ in terms of measured profiles $\tilde{\varepsilon}(\theta)$ and $\tilde{\sigma}(\theta)$. The relation (36) may also be derived directly from the expressions $(33)_1$ and $(34)_1$.

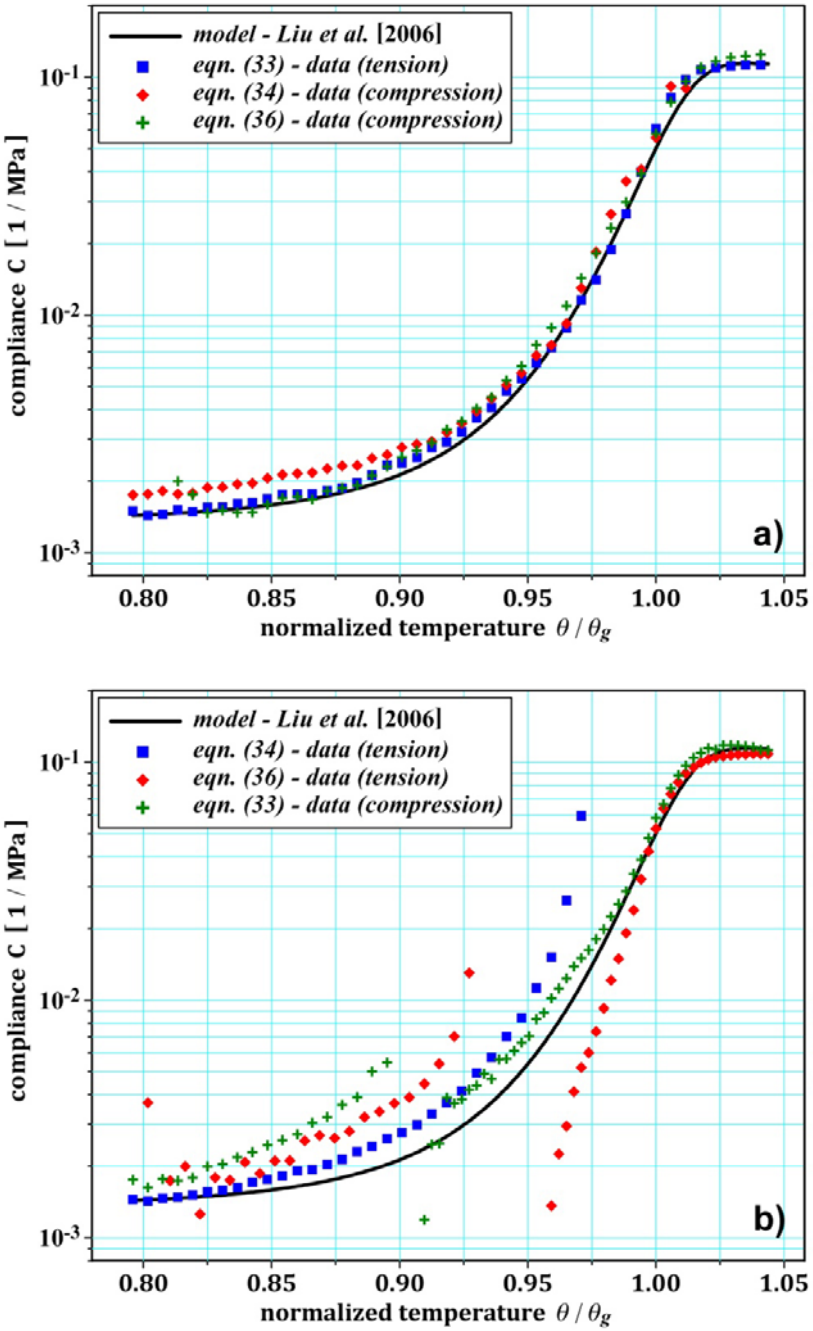

Fig. 8 Elastic compliance C computed from Liu et al. [18, 19] data using the different formulae.

The elastic compliance $C(\theta)$ computed from the data obtained by Liu et al. [19] using equations $(33)_1$, $(34)_1$ and (36) are shown in Fig. 8. The scatter of computed values seen in Fig. 8b is, at least partially, due to digitalization error and possibly due to measurements inaccuracy. Moreover, it

must be noted that equations (34) and (36) require the division by values close to zero and this is the main source of the observed scatter. Furthermore, the determination of the response function $D(\theta)$ from measured profiles requires the computation of derivative of the measured strain recovery profile and this is always problematic when data are given at discrete points. Nevertheless, there is seen in Fig. 9 a fairly good coincidence of the distributed elastic compliance computed from data with theoretical results according to the formula $(12)_1$ for the Liu et al. [18, 19] model.

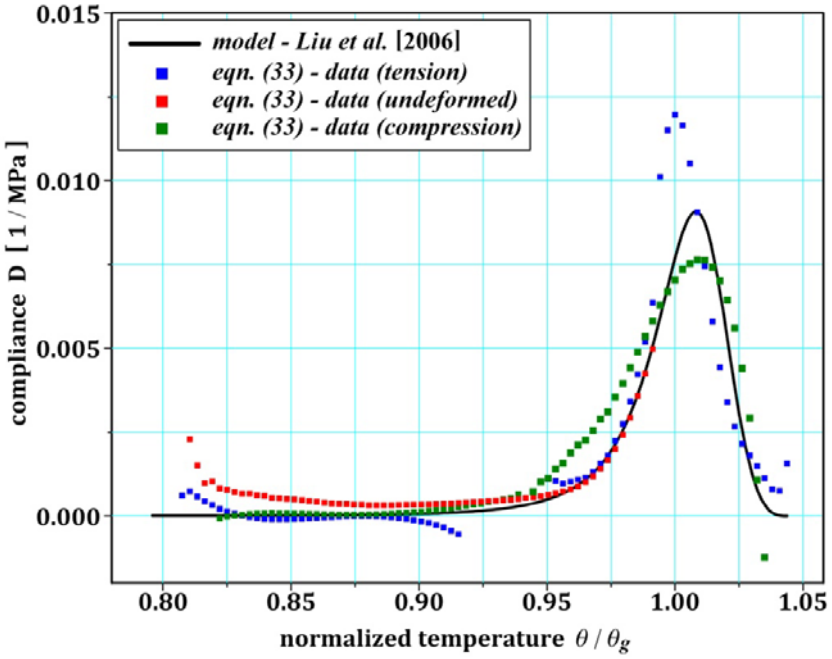

Fig. 9 Elastic compliance D computed from Liu et al. [18, 19] data using formula (33).

The response functions $C(\theta)$ and $D(\theta)$ determined either from the relations (33), (34) or (36) may next be used in numerical simulation of the shape memory behavior of polymers using the general constitutive law (8). For the successive steps of SMCs, this law requires the solution of the integral-differential equation, which may be reduced to the solution of the initial value problem for a first order ordinary differential equation.

It should be apparent that if the response functions $C(\theta)$ and $D(\theta)$ determined from data by the method presented above are used in numerical simulations, a better prediction of the stress storage profile $\hat{\sigma}(\theta)$ is to be expected if (34) is evaluated. To obtain a better prediction of the stress recovery profile $\tilde{\sigma}(\theta)$ one should apply equation (36).

Next, the same analysis and corresponding results may be obtained from constitutive relations derived for the stress-controlled SMCs (Section 6.2). Specifically, using constitutive relations (26) and (30) for the Step 2 and Step 4a of the stress-controlled SMC, the instant elastic compliance $C(\theta)$ and the distributed elastic compliance $D(\theta)$ may be expressed in terms of measured profiles as

$$C(\theta)\sigma_m = \hat{\varepsilon}(\theta) - \bar{\varepsilon}(\theta)\,, \qquad D(\theta)\sigma_m = \frac{d\bar{\varepsilon}(\theta)}{d\theta} - \alpha_\theta(\theta)\,. \tag{37}$$

Equivalently, using the constitutive relations (26) and (32) for Step 2 and Step 4b of the stress-controlled SMC, we obtain

$$C(\theta)(\sigma_m - \bar{\sigma}(\theta)) = -(\bar{\varepsilon}_u - \hat{\varepsilon}(\theta)), \qquad D(\theta)\sigma_m = \frac{d\hat{\varepsilon}(\theta)}{d\theta} - \alpha_\theta(\theta) - \left(\frac{dC(\theta)}{d\theta}\right)\sigma_m . \tag{38}$$

Since $\bar{\varepsilon}_u$ and σ_m are measurable quantities while $\hat{\varepsilon}(\theta)$, $\bar{\varepsilon}(\theta)$ and $\bar{\sigma}(\theta)$ are measurable profiles, the relations (37) and (38) allow to determine the response function $C(\theta)$ and $D(\theta)$ from the measured profiles in the stress-controlled SMCs. These response functions may then be used for the numerical simulation of the shape memory behavior of polymers.

As direct implication of $(37)_2$ and $(38)_2$, we have

$$\frac{d}{d\theta}\left(\hat{\varepsilon}(\theta) - \bar{\varepsilon}(\theta)\right) = \frac{d}{d\theta}\left(C(\theta)\sigma_m\right). \tag{39}$$

The integration of (39) in the temperature sub-interval $[\theta_l, \theta] \subset [\theta_l, \theta_h]$ corresponding to the fourth step of the stress-controlled SMCs with $\hat{\varepsilon}(\theta_l) = \varepsilon_l$ and $\bar{\varepsilon}(\theta_l) = \bar{\varepsilon}_u$ gives

$$(\varepsilon_l - \hat{\varepsilon}(\theta)) - (\bar{\varepsilon}_u - \bar{\varepsilon}(\theta)) = \left(C(\theta_l) - C(\theta)\right)\sigma_m . \tag{40}$$

This is still another relation between strain storage and recovery profiles measured in the stress-controlled SMCs.

The derived results show that the response functions $C(\theta)$ and $D(\theta)$ appearing in the general LTE model may be directly determined from profiles measured in both strain- and stress-controlled SMCs provided that the overall coefficient of thermal expansion $\alpha_\theta(\theta)$ is measured in an independent test. This seemingly simple observation has many far-reaching implications for the evaluation of constitutive models in the LTE class. Unfortunately, no data are yet available in the literature for the stress-controlled SMCs that could be used for this analysis.

8. Universal relations and model's evaluation

The macroscopically observed shape memory effect in polymeric materials is thought to be related to temperature-dependent changes in the network structure and polymer chain mobility, which take place at micro- to nanoscale [2-6, 8, 9]. Although these processes are not yet fully understood and a consistent picture of the molecular mechanisms determining the shape memory effect does not exist, it should be apparent that these mechanisms are independent of the particular type of macroscopic shape memory cycles (SMCs) used to demonstrate this effect. Hence, it may be stipulated that there must exist certain relationships between storage/recovery profiles measured in all four types of SMCs discussed in Section 2. To find such relationships experimentally seems to be a hopeless task, but the theoretical analysis of linear thermoelastic (LTE) models for SMPs presented above gives an interesting insight into possible formulations of such relations.

From equations (33) and (36) for the response functions $C(\theta)$, we have the following relationship

$$\tilde{\sigma}(\theta)(\varepsilon_m - \tilde{\varepsilon}(\theta)) = \hat{\sigma}(\theta)(\varepsilon_u - \tilde{\varepsilon}(\theta)) \tag{41}$$

between the strain and stress profiles $\hat{\sigma}(\theta)$, $\tilde{\varepsilon}(\theta)$ and $\tilde{\sigma}(\theta)$ measured in the strain-controlled SMCs in the free and constrained recovery. As a simple illustration of the importance of the derived result (41), let us note that the following relationship

$$\rho_\sigma \equiv \frac{\tilde{\sigma}(\theta)}{\hat{\sigma}(\theta)} = \rho_\varepsilon \equiv \frac{\varepsilon_u - \tilde{\varepsilon}(\theta)}{\varepsilon_m - \tilde{\varepsilon}(\theta)} \tag{42}$$

must be satisfied for all experimentally determined strain and stress profiles $\hat{\varepsilon}(\theta)$, $\hat{\sigma}(\theta)$ and $\tilde{\sigma}(\theta)$. This theoretical relation (42) may be used in two different ways.

If the strain and stress profiles are experimentally determined, then the relation (42) serves to verify the applicability of the LTE constitutive model. Fig. 10 shows the stress and strain ratio ρ_σ and ρ_ε calculated from Liu et al. [19] data. It could be observed that the theoretical relation (42) is reasonably well satisfied and this proves the approximate applicability of the LTE model to describe the polymer tested by Liu et al.

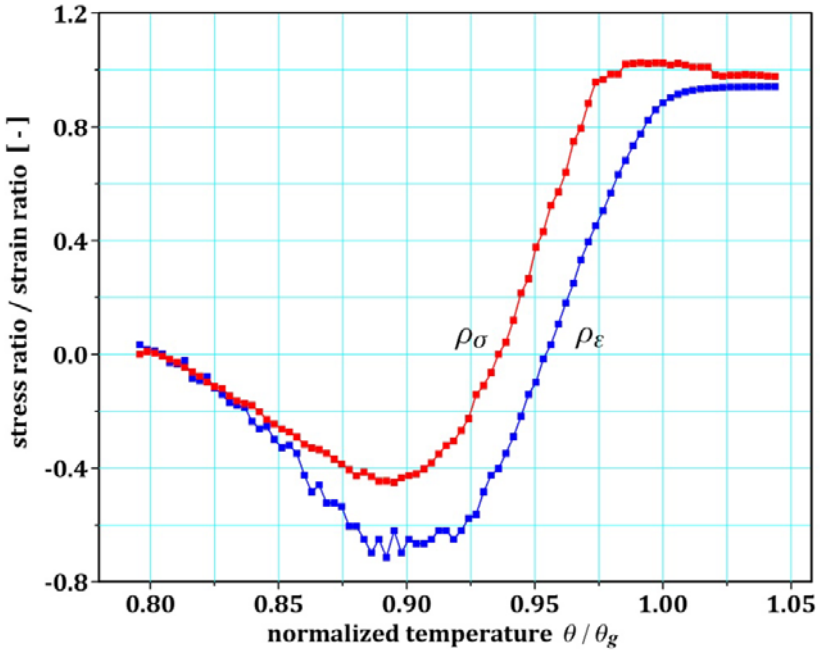

Fig. 10. Comparison of stress and strain ratio defined in (42) for Liu et al. [19] data in tension.

On the other hand, assuming the applicability of the theoretical relation (42) for the considered polymer, any of the strain or stress profiles $\hat{\varepsilon}(\theta)$, $\hat{\sigma}(\theta)$ or $\tilde{\sigma}(\theta)$ may be determined from the other two:

$$\tilde{\sigma}(\theta) = \hat{\sigma}(\theta)\frac{\varepsilon_u - \tilde{\varepsilon}(\theta)}{\varepsilon_m - \tilde{\varepsilon}(\theta)}, \qquad \hat{\sigma}(\theta) = \tilde{\sigma}(\theta)\frac{\varepsilon_m - \tilde{\varepsilon}(\theta)}{\varepsilon_u - \tilde{\varepsilon}(\theta)}. \tag{43}$$

This is illustrated in Fig. 11. It follows that only two profiles need to be experimentally measured for the determination of response functions in the LTE model.

In the same way, from the formulae (37) and (38) for $C(\theta)$, we obtain the relationship

$$(\sigma_m - \bar{\sigma}(\theta))(\hat{\varepsilon}(\theta) - \bar{\varepsilon}(\theta)) = -\sigma_m(\bar{\varepsilon}_u - \hat{\varepsilon}(\theta)) \tag{44}$$

between the strain and stress profiles $\hat{\varepsilon}(\theta)$, $\bar{\varepsilon}(\theta)$ and $\bar{\sigma}(\theta)$ measured in the free and constrained recovery of the stress-controlled SMCs.

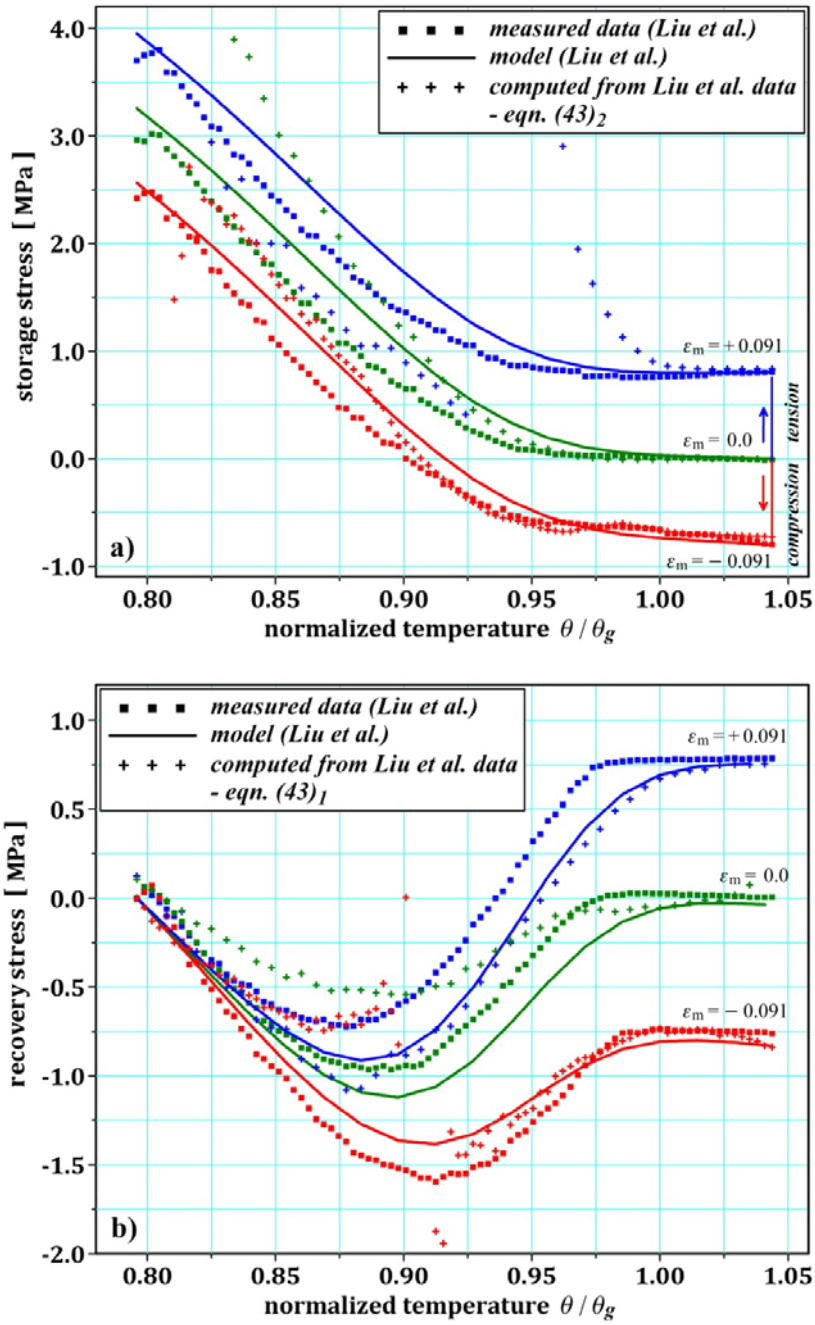

Fig. 11. Comparison of storage and recovery stress.

The relationships (41) and (44) must be satisfied within the strain- and stress-controlled SMCs, respectively. Furthermore, using the formulae (33), (34), (37) and (38), four additional relationships between measured profiles in both tests simultaneously may be obtained

$$\frac{\varepsilon_m - \varepsilon_u}{\hat{\sigma}(\theta) - \tilde{\sigma}(\theta)} = \frac{\hat{\varepsilon}(\theta) - \bar{\varepsilon}(\theta)}{\sigma_m}, \tag{45}$$

$$\frac{\varepsilon_m - \tilde{\varepsilon}(\theta)}{\hat{\sigma}(\theta)} = \frac{\hat{\varepsilon}(\theta) - \bar{\varepsilon}(\theta)}{\sigma_m}, \tag{46}$$

$$\frac{\varepsilon_m - \tilde{\varepsilon}(\theta)}{\hat{\sigma}(\theta)} = -\frac{\bar{\varepsilon}_u - \hat{\varepsilon}(\theta)}{\sigma_m - \bar{\sigma}(\theta)}, \tag{47}$$

$$\frac{\varepsilon_m - \varepsilon_u}{\hat{\sigma}(\theta) - \tilde{\sigma}(\theta)} = -\frac{\bar{\varepsilon}_u - \hat{\varepsilon}(\theta)}{\sigma_m - \bar{\sigma}(\theta)}. \tag{48}$$

It should be noted that the relationships (41) and (44) involve only three profiles while each of the relationships (45) - (48) involve four profiles measured in two different types of SMC tests.

All the relations (41), (44) - (48) are universal in the sense that for any SMP, which may be correctly described by LTE model, the strain/stress storage/recovery profiles measured in SMCs must satisfy (at least approximately) these relations. Their role in the theory of LTE models is analogous to the role of universal relations in the theory of finite elasticity (see Beatty [28], Hayes and Knops [29], Pucci and Saccomandi [30]). In particular, these universal relationships provides the theoretical basis for an experimental validation of the LTE constitutive models.

9. Conclusions

Following the literature on the characterization of SMPs, we have discussed four basic types of SMCs that may be used for the experimental determination of functional properties of these smart materials. It is shown that in all four SMCs there are altogether eight stress/strain storage/recovery profiles that must be experimentally measured besides stress-strain data at high and low temperature. The measured profiles provide experimental foundations for the calibration of constitutive models for SMPs. In the case of LTE model, the independent response functions may be determined in four distinct ways using just two of the eight different stress/strain storage/recovery profiles measured in SMCs. This basic observation may be used for the calibration of the response functions, on the one hand, and for the evaluation of particular models within this class, on the other hand. Finally, we have shown that there are six universal relations between the experimentally measured profiles that must be satisfied by every SMP whose behavior is in agreement with the LTE constitutive model. Their importance lies in the fact that if any such relation cannot be satisfied by data obtained in a suitably designed SMC test of a shape memory polymer, then the behavior of this material cannot be described by any constitutive theory in the LTE class. All models within this class provide computational (theoretical) bases for the simulation of the one-way, two-shape memory effect. To account for time-dependent effects (e.g. holding times), multi-shape effects, and reversible shape changes in polymeric materials more general (visco-thermoelastic) models must be used.

References

[1] Bajpai, A.K.; Bajpai, J.; Saini, R.; Gupta, R.: [2011], Responsive polymers in biology and technology. Polymer Reviews, Vol. 51, Issue 1, pp. 53-97.

[2] Behl, M., Lendlein, A., 2007. Shape-memory polymers. Materials Today, Vol. 10, No 4, pp. 20-28.

[3] Hu, J.; Zhu, Y.; Huang, H.; Lu, J.: [2012], Recent advances in shape-memory polymers: Structure, mechanism, functionality, modeling and applications. Progress in Polymer Science, Vol. 37, pp. 1720-1763

[4] Lendlein, A., Behl, M., Hiebl, B., Wischke, C., 2010. Shape-memory polymers as a technology platform for biomedical applications. Expert Review of Medical Devices, Vol. 7, Issue 3, pp. 357-379.

[5] Liu, C., Qin, H., Mather, P.T., 2007. Review of progress in shape-memory polymers. Journal of Material Chemistry, Vol. 17, No 16, pp. 1543-1558.

[6] Mather, P.T., Luo, X., Rousseau, I.A., 2009. Shape memory polymer research. Annual Review of Materials Research 2009, Vol. 39, pp. 445-471.
[7] Quadrini, F.; Santo, L.; Squeo, E.A.: [2012], Shape memory epoxy foams for space applications. Materials Letters, Vol. 69, pp. 20-23.
[8] Ratna, D., Karger-Kocsis, J., 2007. Recent advances in shape memory polymers and composites: A review. Journal of Materials Science, Vol. 43, Issue 1, pp. 254-269.
[9] Rousseau, I.A., 2008. Challenges of shape memory polymers: A review of the progress toward overcoming SMP's limitations. Polymer Engineering and Science, Vol. 48, Issue 11, pp. 2075-2089.
[10] Serrano, M.C.; Ameer, G.A.: [2012], Recent insights into the biomedical applications of shape-memory polymers. Macromolecular Bioscience, Vol. 12, Issue 9, pp. 1156-1171.
[11] Heuchel, M., Sauter, T., Kratz, K., Lendlein, A., 2013. Thermally induced shape-memory effects in polymers: quantification and related modeling approaches. Journal of Polymer Science, Part B: Polymer Physics, Vol. 51, Issue 8, pp. 621-637.
[12] Sauter, T., Heuchel, M., Kratz, K., Lendlein, A., 2013. Quantifying the shape-memory effect of polymers by cyclic thermomechanical tests. Polymer Reviews, Vol. 53, Issue 1, pp. 6-40.
[13] Wagermaier, W., Kratz, K., Heuchel, M., Lendlein, A., 2010. Characterization methods for shape-memory polymers. Advances in Polymer Science, Vol. 226, pp. 97-145.
[14] Gilormini, P., Diani, J., 2012. On modeling shape memory polymers as thermoelastic two-phase composite materials. Comptes Rendus Mécanique, Vol. 340, Issues 4-5, pp. 338-348.
[15] Nguyen., T.D., 2013. Modeling shape-memory behavior of polymers. Polymer Reviews, Vol. 53, Issue 1, pp. 130-152.
[16] Volk, B., 2009. Thermomechanical characterization and modeling of shape memory polymers. Master of Science Thesis, Texas A&M University.
[17] Zhang, Q., Yang, Q.-S., 2012. Recent advance on constitutive models of thermal-sensitive shape memory polymers. Journal of Applied Polymer Science, Vol. 123, Issue 3, pp. 1502-1508.
[18] Liu, Y., Gall, K., Dunn, M.L., Greenberg, A.R., 2005. Thermomechanics of the shape memory effect in polymers. In: Materials Research Society Symposium Proceedings, Vol. 855E, Paper W5.8 (6 pages).
[19] Liu, Y., Gall, K., Dunn, M.L., Greenberg, A.R., Diani, J., 2006. Thermomechanics of shape memory polymers: Uniaxial experiments and constitutive modeling. International Journal of Plasticity, Vol. 22, Issue 2, pp. 279-313.
[20] Chen, Yi.-C., Lagoudas, D.C., 2008. A constitutive theory for shape memory polymers. Part II: A linearized model for small deformations. Journal of Mechanics and Physics of Solids, Vol. 56, Issue 5, pp. 1766-1778.
[21] Li, L., 2008. Constitutive Modeling of Shape Memory Polymers. PhD Thesis Department of Mechanical Engineering, University of Houston, December 2008.
[22] Jarali, C.S., Raja, S., Upadhya, A.R., 2010. Constitutive modeling of SMA SMP multifunctional high performance smart adaptive shape memory composite. Smart Materials and Structures, Vol. 19, Issue 10, pp. 105029 (14pp).
[23] Ryan, E., Quinlan, N., Bruzzi, M., 2010. Finite element implementation of a constitutive behaviour for shape memory polymers. College of Engineering and Informatics, Research Day, April 15th, 2010, Mechanical Research Session.
[24] Husson, J.M., Dubois, F., Sauvat, N., 2011. A finite element model for shape memory behavior. Mechanics of Time-Dependent Materials, Vol. 15, Issue 3, pp. 213-237.
[25] Sinha, R.P., Jarali, C.S., Raja, S., 2011. Modelling the thermomechanical behaviour of shape memory polymer materials. Indian Journal of Engineering and Materials Sciences, Vol. 18, No 1, pp. 15-23.
[26] Siskind, R.D., 2008. Model development for shape memory polymers. PhD theses, Graduate Faculty of North Carolina State University.
[27] Siskind, R.D., Smith, R.C., 2008. Model development for shape memory polymers. In: Behavior and Mechanics of Multifunctional and Composite Materials (Dapino, M.J. and Ounaies, Z., eds), Proceedings of the SPIE, Vol. 6929, pp. 69291H-69291H-10.
[28] Beatty, M.F., 1987. A class of universal relations in isotropic elasticity theory. Journal of Elasticity, Vol. 17, Issue 2, pp. 113-121.

[29] Hayes, M., Knops, R.J., 1966. On universal relations in elasticity theory. Zeitschrift für Angewandte Mathematik und Physik (ZAMP), Vol. 17, No 5, pp. 636-639.
[30] Pucci, E., Saccomandi, G., 1997. On universal relations in continuum mechanics. Continuum Mechanics and Thermodynamics, Vol. 9, Issue 2, pp. 61-72.
[31] Kazakevičiūtė-Makovska, R., Steeb, H., Aydin, A.Ö., 2012. On the evolution law for the frozen fraction in linear theories of shape memory polymers. Archive of Applied Mechanics, Vol. 82, Issue 8, pp 1103-1115.
[32] Kratz, K., Wagermaier, W., Heuchel, M., Lendlein, A., 2010. Thermomechanical characterizations of shape-memory polymers (dual/triple-shape) and modeling approaches. In: Shape-Memory Polymers and Multifunctional Composites (J. Leng and Y. Liu, eds), pp. 91-107, CRC Press, Taylor and Francis Group.